THE JOURNAL OF PHYSICAL CHEMISTRY B

Article

pubs.acs.org/JPCB

Effect of Molecular Architecture of PDMAEMA–POEGMA Random and Block Copolymers on Their Adsorption on Regenerated and Anionic Nanocelluloses and Evidence of Interfacial Water Expulsion

Maija Vuoriluoto,[†] Hannes Orelma,[*,†,‡] Leena-Sisko Johansson,[†] Baolei Zhu,[§] Mikko Poutanen,[∥] Andreas Walther,[§] Janne Laine,[†] and Orlando J. Rojas[†]

[†]Biobased Colloids and Materials group (BiCMat), Department of Forest Products Technology, School of Chemical Technology, Aalto University, FI-00076, Espoo, Finland

[‡]VTT, Technical Research Centre of Finland, Biologinkuja 7, P.O. Box 1000, FIN-02044 VTT, Finland

[§]DWI – Leibniz-Institute for Interactive Materials Research, Forckenbeckstr. 50, D-52056 Aachen, Germany

[∥]Department of Applied Physics, School of Science, Aalto University, FI-00076, Espoo, Finland

Supporting Information

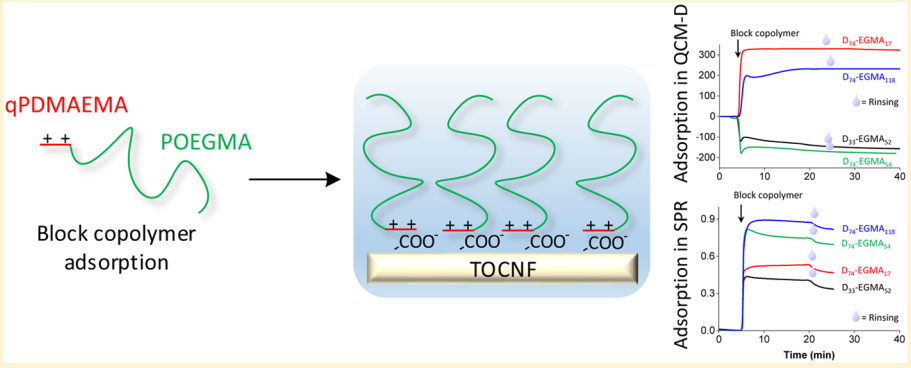

ABSTRACT: Block copolymers of poly(2-(dimethylamino)ethyl methacrylate) (PDMAEMA) and poly(oligo(ethylene glycol) methyl ether methacrylate) (POEGMA) with varying block sizes were synthesized by consecutive reversible addition–fragmentation chain transfer (RAFT) polymerization and then exposed to cellulose substrates with different anionic charge density. The extent and dynamics of quaternized PDMAEMA-*b*-POEGMA adsorption on regenerated cellulose, cellulose nanofibrils (CNF), and (2,2,6,6-tetramethylpiperidin-1-yl)oxyl (TEMPO)-oxidized cellulose nanofibrils (TOCNF) was determined by using electromechanical and optical techniques, namely, quartz crystal microbalance (QCM-D) and surface plasmon resonance (SPR), respectively. PDMAEMA-*b*-POEGMA equilibrium adsorption increased with the anionic charge of cellulose, an indication of electrostatic interactions. Such an observation was further confirmed by atomic force microscopy (AFM) and X-ray photoelectron spectroscopy (XPS). Depending on their architecture, adsorption on TOCNF of some of the PDMAEMA-*b*-POEGMA copolymers produced a significant reduction in QCM frequency, as expected from large mass uptake, while surprisingly, other copolymers induced the opposite effect. This latter, remarkable behavior was ascribed to coupled water expulsion from the interface upon charge neutralization of anionic surface sites with adsorbing cationic polymer segments. These observations were further investigated with SPR and QCM-D measurements using deuterium oxide solvent exchange to determine the amount of coupled water at the TOCNF–block copolymer interface. Finally, random copolymers with similar composition adsorbed to a larger extent compared to the respective block copolymers, revealing the effect of adsorbed loops and tails as well as hydration.

INTRODUCTION

Developing technologies based on renewable materials to support ever increased consumption of carbon-based materials has become increasingly important. Cellulose is a renewable material that can offer solutions to many of these demands. Nanoscale cellulosic materials and specifically cellulose nanofibrils (CNF) have been proposed to improve functionality in many applications as reinforcement agents in composites,[1,2] for fiber technologies,[3] rheology modifiers,[4] absorbent materials,[5] filters,[6] diagnostic systems,[7,8] and barrier films.[9] CNF is typically extracted from plant biomaterial through mechanical[4,10] or chemical[11,12] treatments. CNF also displays a large water uptake ability and a tendency to form hydrogels due to physical and chemical cross-linking.[11] Therefore, the wide application field of

Received: August 6, 2015
Revised: November 3, 2015
Published: November 11, 2015

DOI: 10.1021/acs.jpcb.5b07628
J. Phys. Chem. B 2015, 119, 15275–15286

Scheme 1. Molecular Structure of Quaternized PDMAEMA−POEGMA Copolymers (a) and Schematic Illustration of the Block Copolymer (b) and Random Copolymer (c) Adsorption on Highly Charged TEMPO-Oxidized CNF (TOCNF) Substrate

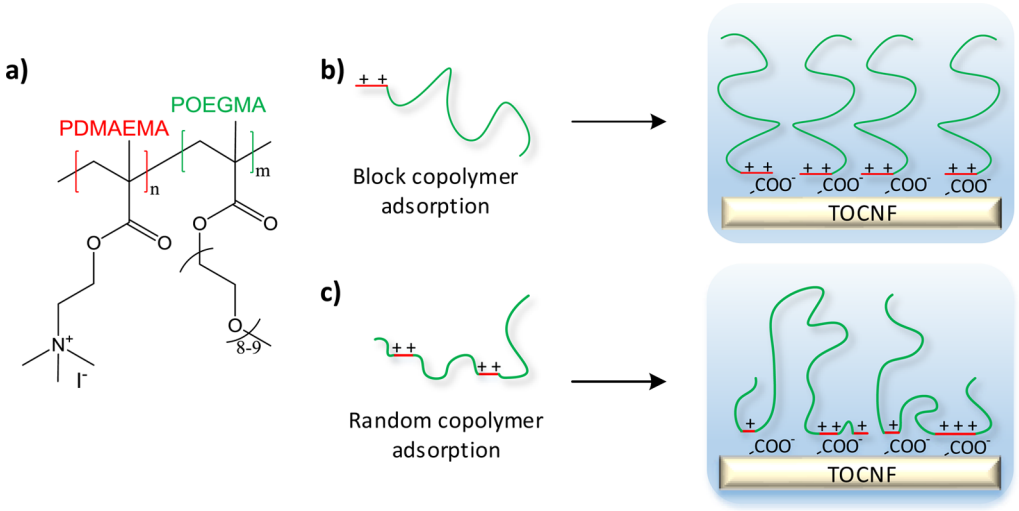

nanocellulose requires a better understanding of its inherent properties and interaction with water, especially if its chemical features are changed via physical or chemical modification.

One simple and effective way for altering the surface chemistry of cellulose is through adsorption of functional surfactants and polymers. We have investigated the adsorption on cellulose of nonionic block copolymers[13−16] as well as triblock copolymers end-capped with cationic chains.[17] Likewise, the attachment on hydrophilic surfaces of copolymers containing cationic poly(2-(dimethylamino)ethyl methacrylate) (PDMAEMA) with hydrophobic segments has been reported, and the adsorption mechanism has been attributed to electrostatic interactions between the cationic segments and the anionic surface, both for quaternized[18] or nonquaternized[19] PDMAEMA. In this work, we study the adsorption on cellulose of similar but entirely hydrophilic copolymers, carrying blocks of positively charged PDMAEMA[20] and highly hydrophilic poly(oligo(ethylene glycol) methyl ether methacrylate) (POEGMA). The cationic PDMAEMA block was hypothesized to function as an anchor for POEGMA onto CNF. Noteworthy, polyethylene glycol molecules (PEG) do not have a high affinity with cellulose[21] but the attachment of PEG on cellulosic material through various indirect routes has been demonstrated.[22,23] CNF modified with block copolymers with PEG-like molecules, which are highly hydrophilic and are in extended conformation in the surrounding aqueous media, find use to stabilize dispersions[24] and provide surface passivation toward nonspecific biomolecule adsorption.[25] Additionally, PEG molecules can supply lubrication in an aqueous environment[26,27] especially relevant to food, pharmaceutical,[28] and biomedical[29] materials. Recently, multifunctional polymers containing PEG molecules have been demonstrated to function as promising antifouling agents toward proteins.[30] Therefore, these entirely hydrophilic block copolymers could potentially be effective in producing antibiofouling cellulose surfaces. Triblock PDMAEMA-*b*-POEGMA-*b*-PDMAEMA copolymers may offer interesting cross-linking options compared to block PDMAEMA-*b*-POEGMA polymers. On the other hand, nonionic symmetric triblock copolymers (such as Pluronics), which are expected to be effective in antifouling, adsorb weakly and only to a limited extent on cellulose.[16] To study the effect of molecular architecture on adsorption and layer properties, random copolymers of DMAEMA and OEGMA were investigated here for this purpose.

CNF−water interactions have a major influence in many related applications due to high water uptake ability and hydrogel formation. One of the consequences of this behavior is that, unless a judicious change in CNF charge density is applied, only limited dispersion in aqueous media occurs once it has been dried.[31] Thus, CNF applications can be highly susceptible depending on its exposure to water, humid air, etc. Relevant to the present investigation are the available ultrathin films of cellulose, which can be studied with surface-sensitive techniques to unveil fundamental aspects of cellulose−water interactions as well as surface (physical and chemical) modification.

Interactions of the cellulose polymer with water have already been extensively investigated;[32,33] recently the interactions between CNF and water have been at the center of interest given its significance in application development. The swelling of CNF ultrathin films in water[34,35] and water uptake of CNF multilayers[36] has been reported. Interestingly, it was found that cationic polyelectrolyte adsorption can reduce swelling of CNF in water.[35] Therefore, the impact on water interactions upon adsorption on cellulose nanofibrils (CNF) and (2,2,6,6-tetramethylpiperidin-1-yl)oxyl (TEMPO)-oxidized CNF (TOCNF) of highly hydrophilic block copolymers containing cationic segments is elucidated in this study. A H_2O/D_2O solvent exchange method in QCM-D[37] was applied for this purpose, as it allows one to determine swelling of regenerated cellulose, cellulose nanocrystals,[38] and CNF[35] films. To this end, the adsorption of block copolymers containing quaternized PDMAEMA and POEGMA on low-charged regenerated cellulose, medium-charged CNF, and highly charged TOCNF was investigated *in situ* by quartz crystal microbalance with dissipation (QCM-D) monitoring[39] and surface plasmon resonance (SPR).[40] QCM-D experiments with H_2O/D_2O solvent exchange were applied to determine the water content of TOCNF films before and after block copolymer adsorption. The changes in topography and surface chemical composition were determined by atomic force microscopy (AFM) and X-ray photoelectron spectroscopy (XPS), respectively. To study the effect of molecular architecture on adsorption, random copolymers of PDMAEMA and POEGMA were adsorbed on TEMPO-oxidized CNF. Scheme 1 illustrates a schematic

DOI: 10.1021/acs.jpcb.5b07628
J. Phys. Chem. B 2015, 119, 15275−15286

representation of PDMAEMA−POEGMA block and random copolymer structure and adsorption on highly charged TOCNF.

EXPERIMENTAL SECTION

Materials. Cellulose nanofibrils (CNF) were produced by processing bleached sulphite birch fibers through a Masuko grinder (three passes) after which they were further microfluidized (at least 12 passes) through a M110P fluidizer (Microfluidics Corp., Newton, MA, USA) equipped with 200 and 100 μm chambers and operated at 2000 bar pressure. Trimethylsilylcellulose (TMSC) was synthesized as previously described.[41] All used laboratory chemicals were of analytical grade. Deionized water further purified with a Millipore Synergy UV unit (Milli-Q) was used in all experiments.

Reversible Addition−Fragmentation Chain Transfer (RAFT) Polymerization of PDMAEMA. A 1.65 g portion of DMAEMA (2-(dimethylamino)ethyl methacrylate, 10.5 mmol) and 14.1 mg (0.51 mmol) of 4-cyano-4-(phenylcarbonothioylthio) pentanoic acid was weighed and dissolved in 8 mL of 1,4-dioxane in a container with a stirrer. Afterward, 2.5 mg (0.015 mmol) of 2,2′-azobis(2-methylpropionitrile) was added, and the container was sealed with a rubber septum and bubbled with N_2 for 20 min to remove oxygen. The container was placed into an oil bath at 70 °C. Samples were taken during the reaction to monitor conversion and molecular weight evolution. After 15 h, the reaction system was cooled down in an ice bath. The polymer was precipitated in hexane at least three times to remove the unreacted monomer and freeze-dried to yield a pure polymer. PDMAEMA precursors with different molecular weights were made.

Chain Extension of PDMAEMA to PDMAEMA-*b*-POEGMA. The chain extension of PDMAEMA to PDMAEMA-*b*-POEGMA was carried out in a similar manner as RAFT polymerization of PDMAEMA. A 2.5 g portion of OEGMA (oligo(ethylene glycol) methyl ether methacrylate, 5.3 mmol) and 0.169 g of PDMAEMA precursor (0.0212 mmol) was weighed and dissolved in a container with a stirrer. Afterward, 0.7 mg of AIBN (0.0042 mmol) was added, and the container was sealed with a rubber septum and bubbled with N_2 for 20 min to remove oxygen. The container was placed into an oil bath at 65 °C. Samples were taken during the reaction to monitor the conversion and molecular weight. After 7 h, the reaction system was cooled down in an ice bath. The polymers were dialyzed against water for 7 days and freeze-dried to yield the purified polymers.

The samples were quaternized by dissolving 1 g of block copolymer in 15 mL of 1,4-dioxane in a vial with a stirrer. Afterward, 0.52 mL of methyl iodide was added into the polymer solution in a quick manner while keeping the solution stirring rigorously. After 24 h, the quaternization reaction was complete. The polymer solution was freeze-dried to get rid of the solvent and residual methyl iodide. A yellowish powder was yielded.

Characterization of PDMAEMA-*b*-POEGMA. ^{1}H NMR spectra (400 MHz) of the polymers were recorded using a Bruker DPX 400 instrument. All spectra were referenced internally to residual proton signals of the deuterated solvent ($CDCl_3$). SEC with DMF (HPLC grade, VWR) as eluent was performed using an Agilent 1100 system equipped with a dual RI-/Visco detector (ETA-2020, WGE). The eluent contained 1 g·L^{-1} LiBr (≥99%, Sigma-Aldrich). The sample solvent contained traces of distilled water as internal standard. One precolumn (8 × 50 mm) and four GRAM gel columns (8 × 300 mm, Polymer Standards Service) were applied at a flow rate of 1.0 mL·min^{-1} at 40 °C. The diameter of the gel particles measured 10 μm, and the nominal pore widths were 30, 100, 1000, and 3000 Å. Calibration was achieved using narrow distributed poly(methyl methacrylate) standards (Polymer Standards Service).

The as-prepared PDMAEMA-*b*-POEGMA copolymers contained varying DMAEMA and OEGMA repeating units: 33, 58, or 74 for DMAEMA and 10 to 137 for OEGMA. A total of nine block copolymers combining these block sizes were used and referred to as D_n-$EGMA_m$, where n and m represent the number of DMAEMA and OEGMA units in the copolymer, respectively.

In addition, four random copolymers of PDMAEMA and POEGMA (PDMAEMA-*rnd*-POEGMA) with well-defined molar percentage ratios (10−90, 30−70, 70−30, 90−10) were synthesized by ATRP and quaternized by methyl iodide.

Preparation of Cellulose Substrates. Regenerated cellulose, cellulose nanofibrils (CNF), and TEMPO-oxidized CNF (TOCNF) were utilized in the form of ultrathin films that were used as adsorbing substrate. All of the cellulose films were stored under ambient conditions and were allowed to stabilize in water overnight prior to measurements in QCM-D or SPR (see methods further below).

Regenerated cellulose thin films were deposited on QCM-D silica crystals (Q-Sense, Västra Frölunda, Sweden) from TMSC according to Kontturi et al.[42] The QCM-D crystals were first cleaned with UV/ozone treatment for 20 min and subsequently spin-coated (model WS-650SX-6NPP, Laurell Technologies, PA, USA) at 4000 rpm for 60 s with a 10 g/L solution of TMSC in toluene. The TMSC surfaces were hydrolyzed to regenerated cellulose by a hydrochloric acid vapor treatment.

CNF thin films were prepared according to Ahola et al.[43] In short, CNF gel was diluted (0.190 wt % CNF in water) and tip-ultrasonicated for 10 min at 25% amplitude setting and consecutively centrifuged at 10400 rpm for 45 min. Individual nanofibrils were obtained from the resultant clear supernatant. The nanofibrils were spin-coated onto UV/ozonized silica QCM-D or gold SPR (Oy BioNavis Ltd., Ylöjärvi, Finland) wafers with a preadsorbed thin anchor layer of PEI at 3000 rpm with 90 s spinning time. After spin-coating, the CNF films were dried at 80 °C for 10 min.

CNF films were TEMPO-oxidized *in situ* in the QCM-D and SPR modules, thereby introducing carboxylic groups on the surface. The oxidation process was monitored in real time in the QCM and SPR setups (see Supporting Information S1 for the typical QCM-D and SPR sensograms upon TEMPO oxidation of CNF films). In short, CNF films were subjected to continuous flow of TEMPO solution (0.13 mmol of TEMPO, 4.65 mmol of NaBr, and 5.00 mmol of NaClO in water, pH 10) for 2 min after which oxidation was stopped by ethanol addition for 2 min. Milli-Q-water rinsing was applied to remove any excess oxidation chemicals. Subsequently, the films were allowed to stabilize in 2.5 mM phosphate buffer solution at pH 6.8 (ionic strength 4 mM) and they were used for block copolymer adsorption measurements immediately without drying steps.

Quartz Crystal Microbalance with Dissipation (QCM-D). The adsorption of the block and random copolymers on regenerated cellulose, CNF, and TOCNF films were monitored with a Q-Sense E4 apparatus (Västra Frölunda, Sweden). The QCM-D technique is based on the acoustic oscillation of a quartz crystal by which adsorption events can be monitored.[39] The dissipation values measured simultaneously yield information about the viscoelastic properties of adsorbing layers.[44] The frequency and dissipation changes were measured at a fundamental resonance frequency and its overtones. In an ideal

DOI: 10.1021/acs.jpcb.5b07628
J. Phys. Chem. B 2015, 119, 15275−15286

case, the adsorbed mass is proportional to the change in resonance frequency according to the Sauerbrey equation[45,46]

$$\Delta m = -C_{\text{QCM-D}}\frac{\Delta f}{n} \tag{1}$$

where $C_{\text{QCM-D}}$ is 17.7 ng Hz^{-1} cm^{-2} for 5 MHz crystal (provided by the manufacturer), Δf is the change in frequency, and n corresponds to the overtone number. The Sauerbrey equation is applicable only if the adsorbed layer is uniformly distributed on the crystal surface, it is rigid, and the mass is small compared to the mass of the crystal; if these conditions are not fulfilled, the calculation results in mass overestimation. Under such conditions, the Voigt viscoelastic model is more appropriate. Therefore, we used the Voigt protocol (Q-Tools software, version 2.1, Q-Sense, Västra Frölunda, Sweden) to estimate the adsorbed mass of block copolymers on the surfaces by assuming a density of 1200 g/m^3 for the adsorbed layer.[47] All QCM-D experiments were repeated at least twice under a constant flow rate of 100 μL/min at 23 °C.

Determination of Coupled Water with H_2O/D_2O Solvent Exchange in QCM-D. QCM-D was also utilized to determine the mass of spin-coated CNF on the silica sensor crystal by comparing the recorded fundamental resonance frequency of the sensor in air before and after CNF deposition. The water content of CNF and TOCNF films was determined according to a previously published method,[37,38] by changing the water solvent to deuterium oxide (D_2O) and comparing the scaled QCM-D frequency shift. The contribution of bound water within the film $(\Delta f/n)_{H_2O}$ can be calculated from eq 2[38,48]

$$\left(\frac{\Delta f}{n}\right)_{H_2O} = \frac{\left(\frac{\Delta f}{n}\right)_{\text{film}} - \left(\frac{\Delta f}{n}\right)_{\text{bare}}}{\left(\frac{\rho_{D_2O}}{\rho_{H_2O}}\right) - 1} \tag{2}$$

where $(\Delta f/n)_{\text{film}}$ is the scaled frequency shift measured when the CNF or TOCNF film is changed from H_2O to D_2O, $(\Delta f/n)_{\text{bare}}$ is the scaled frequency shift measured when the bare silica sensor is switched from H_2O to D_2O, and ρ_{H_2O} and ρ_{D_2O} are the densities at 20 °C of the solvents (0.9982 and 1.1050 g/cm^3 for H_2O[49] and D_2O,[50] respectively). The total water content of the film was then calculated according to eq 1. Prior to solvent exchange, CNF films were allowed to swell in Milli-Q water overnight. When a stable baseline at a constant flow of 100 μL/min (T = 20 °C) was reached, the solvent was exchanged to D_2O and the frequency shift was monitored. After 10 min, the solvent was changed back to Milli-Q water and the frequency returned back to the initial baseline. This procedure was repeated after *in situ* TEMPO oxidation of the CNF films. The effect of block copolymer adsorption on the water content of the TOCNF was investigated by studying the H_2O/D_2O solvent exchange responses before and after the adsorption of the polymer.

Surface Plasmon Resonance (SPR). Block copolymer adsorption on TOCNF was monitored in real time with a multiparametric surface plasmon resonance instrument (MP-SPR Model Navi 200, Oy BioNavis Ltd., Ylöjärvi, Finland). The SPR effect involves a sharp attenuation of light reflectivity caused by a loss of energy associated with coupling of the directed light with surface plasmon waves traveling along the analyzed solution and solid layer interface. As a result, changes occur in the reflected light energy and angles of maximum reflection intensity.[40] The refractive indexes (RI) of media in contact with the surface of the SPR crystal correlate very sensitively with the angles and wavelengths at which the surface plasmon resonance effect occurs.[51,52] Equation 3 was used to determine the thickness of the adsorbed layer[51]

$$d = \frac{l_d}{2}\frac{\Delta_{\text{angle}}}{m(n_a - n_0)} \tag{3}$$

where Δ_{angle} is the change in the SPR angle, l_d is a characteristic evanescent electromagnetic field decay length, estimated as 0.37 of the light wavelength (240 nm), m is a sensitivity factor for the sensor obtained after calibration of the SPR (109.94°/RIU), n_0 is the refractive index of the bulk solution (1.334 RIU), and n_a is the refractive index of the adsorbed substance. The refractive index was estimated as 1.46 for the block copolymers (based on POEGMA).[53] The adsorbed amounts per unit area were calculated following eq 4[52]

$$\Delta m = d \times \rho \tag{4}$$

where d is the thickness of the adsorbed layer and ρ is the packing density of the adsorbed species. The assumed packing density was 1.15 g/cm^3 based on POEGMA[54] for the block copolymers. All SPR measurements were conducted with a 100 μL/min flow rate at 20 °C. Each SPR measurement was performed at least twice.

Adsorption of Block Copolymers on Cellulose Films. The adsorption of nine block copolymers with varying block sizes on regenerated cellulose, CNF, and TOCNF was studied with QCM-D and SPR. The block copolymers (0.5 g/L concentration) were adsorbed on the cellulose surfaces from 2.5 mM phosphate buffer solution at pH 6.8 until an adsorption plateau was observed. Upon reaching equilibrium, rinsing was applied with the respective buffer solution.

Adsorption of Random Copolymers on TOCNF Films. Nonquaternized and quaternized random copolymers with given PDMAEMA-to-POEGMA ratios (10−90%, 30−70%, 70−30%, 90−10%) were adsorbed onto TOCNF films, and the adsorption was monitored via SPR. The nonquaternized versions of the random copolymers were adsorbed onto TOCNF from pH 5.5 acetate buffer solution (10 mM) and from pH 9.5 carbonate buffer solution (10 mM). Likewise, the quaternized polymers were applied onto TOCNF from neutral pH, Milli-Q-water. Rinsing was applied with the respective (background) solvent once the adsorption plateau was reached for the nonquaternized samples and after ∼50 min of adsorption in the case of quaternized samples.

Atomic Force Microscopy (AFM). Changes in surface topography of dried cellulose films with and without adsorbed block copolymers were analyzed with a Nanoscope IIIa multimode scanning probe microscope (Digital Instruments, Santa Barbara, CA). Surface areas of 5 × 5 and 1 × 1 μm^2 were scanned in air using tapping mode with silicon cantilevers; at least three separate areas on each sample were imaged. Flattening was the only image processing step applied.

X-ray Photoelectron Spectroscopy (XPS). The surface chemical composition of the dried cellulose films with and without adsorbed block copolymers was examined with an AXIS Ultra spectrometer by Kratos Analytical using an X-ray source of monochromatic Al Kα at 100 W irradiation under neutralization. Prior to the measurements, the dried but hygroscopic samples were evacuated overnight. A standard *in situ* reference (cellulose) was measured with each sample batch in order to monitor experimental conditions. High resolution spectra of carbon (C 1s), oxygen (O 1s), and nitrogen (N 1s) were recorded in

DOI: 10.1021/acs.jpcb.5b07628
J. Phys. Chem. B 2015, 119, 15275−15286

Table 1. Summary of Molecular Structure Characteristics of Poly(2-(dimethylamino) ethyl methacrylate)-*block*-Poly(oligo(ethylene glycol) methyl methacrylate) (PDMAEMA-*b*-POEGMA) Copolymers[a]

	weight fraction		polymerization degree				
sample code	PDMAEMA	POEGMA	DMAEMA	OEGMA	Mn_{calc} (Da)	Mn_{GPC} (Da)	PDI
D_{33}-$EGMA_{52}$	17	83	33	52	29900	19000	1.21
D_{33}-$EGMA_{94}$	10	90	33	94	49800	36600	1.13
D_{33}-$EGMA_{137}$	7	93	33	137	70300	58400	1.29
D_{58}-$EGMA_{10}$	66	34	58	10	13860	17100	1.20
D_{58}-$EGMA_{62}$	24	76	58	62	38560	35900	1.25
D_{58}-$EGMA_{118}$	14	86	58	118	65156	49200	1.23
D_{74}-$EGMA_{17}$	59	41	74	17	19690	17100	1.17
D_{74}-$EGMA_{54}$	31	69	74	54	37268	31400	1.27
D_{74}-$EGMA_{118}$	17	83	74	118	67668	51300	1.29

[a]Besides the respective polymer sample code, the data include the weight fraction, polymerization degree, calculated molecular weight based on MALDI-TOF and ^{1}H NMR (Mn_{calc}), as well as molecular weight based on GPC (Mn_{GPC}) and respective polydispersity indices.

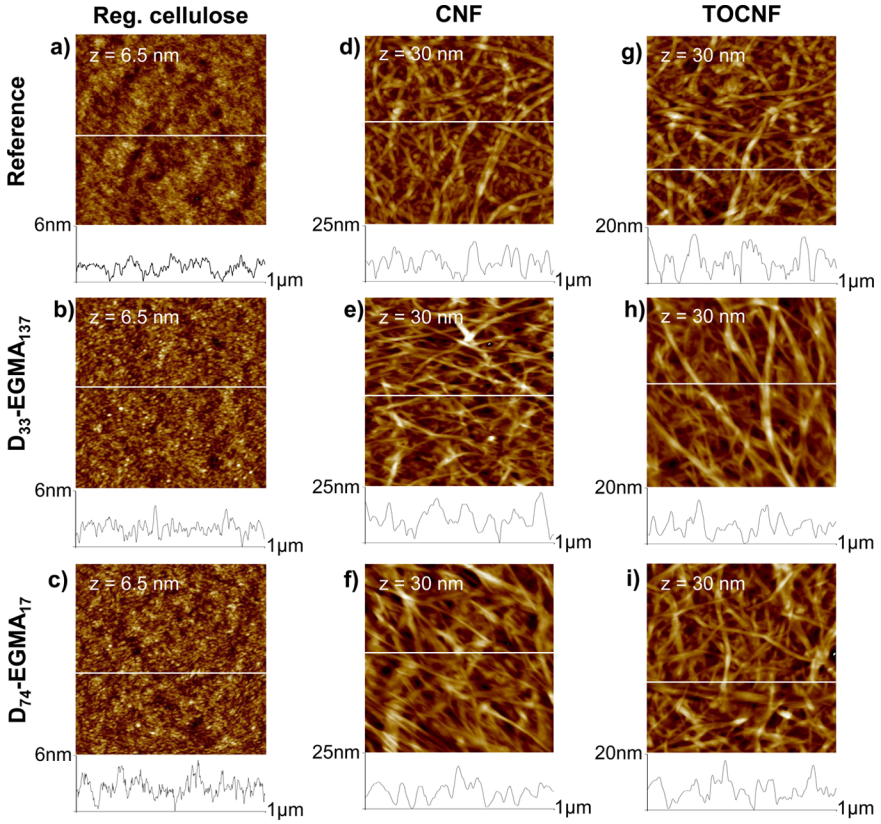

Figure 1. AFM height images 1 × 1 μm^2 of regenerated cellulose, CNF, and TOCNF surfaces before (a, d, g) and after adsorption of D_{33}-$EGMA_{137}$ (b, e, h) and D_{74}-$EGMA_{17}$ (c, f, i) block copolymers (as indicated on the left). The roughness profiles are included in the bottom of the respective image. The subscript in the polymer descriptor refers to the size of PDMAEMA (D) and POEGMA (EGMA) segments.

addition to elemental wide-region data. The analysis area was 400 × 800 μm^2. Sample degradation was not observed during measurements. Detailed descriptions on experimental parameters and high-resolution carbon fits are available elsewhere.[55]

RESULTS AND DISCUSSION

Block Copolymer Samples. The nine block copolymers synthesized for varying block sizes and comprising PDMAEMA (D) and POEGMA (EGMA) were analyzed by MALDI-TOF, ^{1}H NMR, and GPC (Table 1).

Adsorption of PDMAEMA-*b*-POEGMA on Cellulose. The nine PDMAEMA-*b*-POEGMA copolymer samples with varying block sizes were adsorbed onto the cellulose films with different charge density. Figure 1 includes 1 × 1 μm^2 AFM images of D_{33}-$EGMA_{137}$ and D_{74}-$EGMA_{17}$ adsorbed from aqueous solution on films of regenerated cellulose, CNF, and TOCNF followed by air drying (Figure 1a–c, d–f, and g–i, respectively). Images of the respective bare films are included as reference. The AFM images revealed that the CNF and TOCNF reference, bare films (Figure 1d,g) were already initially much rougher than the regenerated cellulose reference (RMS roughness of 3.4, 3.9 and 0.68 nm, respectively). This is due to the fibrillar network structure of CNF. Differences in AFM topography (as determined by RMS roughness) of regenerated cellulose without and with adsorbed block copolymers are rather negligible (Figure 1a–c): the RMS roughness for regenerated

DOI: 10.1021/acs.jpcb.5b07628
J. Phys. Chem. B 2015, 119, 15275–15286

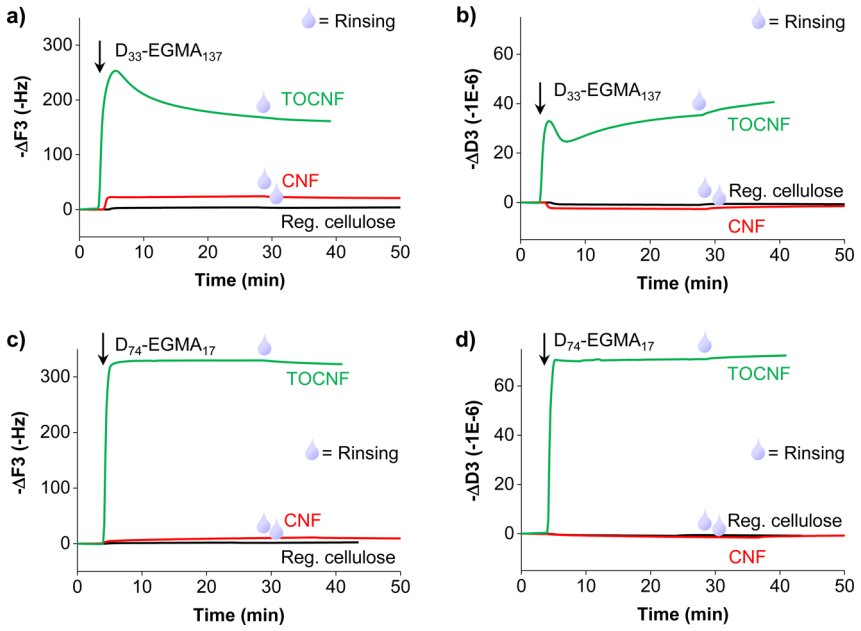

Figure 2. Real time QCM-D shift in frequency, −ΔF3 (a, c), and dissipation, −ΔD3 (b, d), upon D_{33}-$EGMA_{137}$ and D_{74}-$EGMA_{17}$ adsorption on regenerated cellulose, CNF, and TOCNF. The vertical arrows indicate the time at which the block copolymer was introduced in the QCM module, and the droplet symbols indicate rinsing with background solvent (PBS buffer, pH 6.8) at given times after adsorption.

cellulose (0.68 nm, reference) after adsorption of D_{33}-$EGMA_{137}$ and D_{74}-$EGMA_{17}$ is 0.73 and 0.80 nm, respectively. The small changes in roughness indicate negligible effects upon adsorption of the block copolymers on regenerated cellulose. Likewise, adsorption of D_{33}-$EGMA_{137}$ and D_{74}-$EGMA_{17}$ induced no substantial topographical changes on CNF or TOCNF substrates (Figure 1d–i). Altogether, the results from AFM imaging of dried adsorbed layers indicate uniform block polymer adsorption on all tested cellulose surfaces.

The height images of CNF and TOCNF with adsorbed block copolymers in the dry state (Figure 1e,f and h,i) show a fibrillar network structure for both substrates and, also, lower height contrast compared to the respective reference images (Figure 1d and g). This observation in height images of CNF (Figure 1e,f) and TOCNF (Figure 1h,i) carrying the block copolymers can be explained by swelling of the PEG-containing blocks during the relatively humid environment used during AFM imaging. However, the topographical differences between the surfaces are more evident if one compares the RMS values of the respective bare CNF surface (3.4 nm) with those of CNF carrying adsorbed D_{33}-$EGMA_{137}$ and D_{74}-$EGMA_{17}$ (RMS = 4.3 and 4.2 nm, respectively). Analysis of the RMS roughness values for TOCNF surfaces reveals a negligible change in TOCNF film surfaces upon copolymer adsorption, likely the result of uniform binding onto the substrate. Comparatively, the CNF surfaces were subjected to non-negligible changes in RMS roughness, which can be explained to result from nonuniform block copolymer adsorption and/or the presence of coiled chains at the interface. Therefore, there is indication that a more uniform adsorption or a flatter/tighter conformation of block copolymers on the TOCNF surface occurred due to the influence of electrostatic interactions with the cationic segments of the block copolymers. This is in agreement with results from a previous study where PEG molecules were grafted onto carboxymethyl cellulose and adsorbed onto CNF films.[23] We note, however, that the differences in AFM images were rather small and additional inquiries into conformational changes at the interface are needed for more conclusive evidence. Here, QCM-D adsorption experiments with PDMAEMA-*b*-POEGMA block copolymers were carried out on the different cellulose surfaces, with a main emphasis on the adsorbed layer mass and changes in viscoelasticity and water coupling. Thus, AFM imaging before and after adsorption of D_{33}-$EGMA_{137}$ and D_{74}-$EGMA_{17}$ on cellulose (regenerated cellulose, CNF, and TOCNF films) (Figure 1) was taken as complementary to QCM-D experiments (frequency and dissipation) presented in Figure 2, which provided more insightful observations in relation to adsorption phenomena.

The PDMAEMA block contains tertiary amine groups, with a monomer (DMAEMA) pK_a value of ca. 8.4,[20] which means that ∼50% of the amine groups of the monomers are protonated at this pH. Furthermore, reported pK_a values for PDMAEMA of different molecular weight range between 7.4 and 7.8.[20] However, in this work, the tertiary amine groups of PDMAEMA blocks were quaternized (permanent cationic charges) by methylation. As discussed previously, PEG molecules do not have remarkable affinity toward cellulose on their own[21] and the block copolymers in fact adsorb minimally on regenerated cellulose (Figure 2a and c). The adsorption was somewhat higher on CNF and substantially higher, and very fast, on TOCNF. As the CNF surfaces were oxidized *in situ* (inside the QCM-D module) via TEMPO reaction, the traditional methods used to determine surface charge were not applicable; therefore, the charge density of TOCNF films was not accessible. However, such a charge density of cellulose across all experiments involving TOCNF was the same given that the same reaction conditions were used. The pK_a value of carboxylic acids is in the range 3.0–5.5,[56] and hence, the TOCNF is negatively charged at the experimental pH (6.8): this suggests the substantially high adsorption observed on TOCNF is the result of electrostatic interactions (between positively charged PDMAEMA and TOCNF). This is consistent with the existing literature regarding adsorption of PDMAEMA-containing block copolymers on anionic mica, silica, and cellulose surfaces. However, other effects

DOI: 10.1021/acs.jpcb.5b07628
J. Phys. Chem. B 2015, 119, 15275–15286

Table 2. XPS Atomic Concentrations (%) and Standard Deviations (from Analysis of Wide Spectra) for D_{33}-$EGMA_{137}$ and D_{74}-$EGMA_{17}$ Adsorbed on Regenerated Cellulose, CNF, and TOCNF Films[a]

	atomic concentration (%)			
	C 1s	O 1s	N 1s	Si 2p
reg. cellulose (reference)	60.8 ± 0.5	38.2 ± 0.5	0.6 ± 0.5	0.1 ± 0.5
D_{33}-$EGMA_{137}$	62.5 ± 1.0	36.8 ± 0.9	0.6 ± 0.5	N/A
D_{74}-$EGMA_{17}$	62.5 ± 1.2	36.3 ± 1.4	0.7 ± 0.5	0.3 ± 0.5
CNF (reference)	42.4 ± 2.5	41.3 ± 0.9	1.6 ± 0.5	14.9 ± 1.6
D_{33}-$EGMA_{137}$	58.9 ± 1.1	30.6 ± 0.8	5.3 ± 0.8	5.2 ± 0.6
D_{74}-$EGMA_{17}$	60.1 ± 2.1	27.0 ± 0.7	8.3 ± 1.1	4.3 ± 0.5
TOCNF (reference)	43.7 ± 0.9	41.1 ± 0.9	0.9 ± 0.5	14.3 ± 0.5
D_{33}-$EGMA_{137}$	59.0 ± 0.5	30.1 ± 0.6	7.2 ± 0.5	3.7 ± 0.5
D_{74}-$EGMA_{17}$	57.9 ± 0.5	26.4 ± 0.5	13.1 ± 1.0	2.5 ± 0.9
Whatman	60.7 ± 0.6	39.3 ± 0.6	N/A	N/A

[a]Values for reference films are also included as well as a cellulose standard (Whatman filter paper).

may not be discounted in these cases, which involved DMAEMA copolymerized with hydrophobic blocks.[18,19]

The slightly higher adsorption of the block copolymers on CNF compared to regenerated cellulose (Figure 2a and c) can be attributed to the slightly anionic nature of CNF at the adsorption pH ($pK_a \sim 4.8$[36]), resulting from the residual heteropolysaccharides (mainly xylans) that remain on the fibril surfaces from the precursor fibers (delignification and limited removal of hemicelluloses).[56] However, it is also observed that, compared to the case of D_{74}-$EGMA_{17}$, D_{33}-$EGMA_{137}$ adsorbed more extensively on CNF, which highlights the role of the POEGMA segment size and the inherent amount of water coupling.

Noteworthy, the reduction in QCM dissipation values measured upon block copolymer adsorption on TOCNF (Figure 2b and d) indicates that the interface became more rigid. All of the cellulose surfaces investigated experienced substantial swelling in the aqueous environment, and therefore, a stable QCM-D (frequency and dissipation) baseline was ensured before polymer adsorption. This was carried out by allowing the cellulose system to fully swell (overnight equilibration in water and in the QCM-D module). The TOCNF surfaces were therefore fully hydrated prior to QCM-D measurements. The large reduction in dissipation was most likely due to substantial amounts of water released from the TOCNF via charge neutralization. This large water removal was found to cause peculiar frequency changes: adsorption of some of the block copolymers produced an unexpected positive shift in frequency. Since QCM-D measurements are affected by water coupling, the SPR technique was used to shed further light on the process of block copolymer adsorption on TOCNF. As will be introduced later, SPR measurements for all tested block copolymers indicated their irreversible adsorption on TOCNF surfaces. Therefore, it can be concluded that the positive shift in the QCM frequency that was observed is the result of considerable water expulsion from the TOCNF interface, which is driven by charge neutralization during adsorption.

In order to study surface chemical composition, XPS measurements were performed on dried regenerated cellulose, CNF, and TOCNF films, before and after adsorption of D_{33}-$EGMA_{137}$ and D_{74}-$EGMA_{17}$ block copolymers. The XPS wide atomic concentrations for these samples are presented in Table 2 (see Supporting Information S2 for high resolution carbon data). Both wide and high resolution spectra included the typical cellulose signatures.[55] According to the XPS data, the regenerated cellulose films covered the silicon substrate almost completely. Although the CNF and TOCNF films were found to be uniform in AFM (Figure 1d and g), the silicon signal from the substrate was observed for these samples due to contribution from the areas underneath the fibrillar network structure of CNF and TOCNF. XPS analyses are discussed next to determine changes in the composition of the surface upon copolymer adsorption. The nitrogen signal was used as a fingerprint to determine the extent of adsorption for the block copolymers on cellulose.

XPS analysis of the regenerated cellulose films before and after block copolymer adsorption supports the observation of little or no adsorption of the block copolymers on regenerated cellulose: the nitrogen surface concentration remains practically unchanged after adsorption of the polymer. The XPS analysis indicates a small contribution of nitrogen originating from the PEI adsorbed on the crystals, which was used as an anchoring layer for CNF and TOCNF. Block copolymer adsorption on CNF and TOCNF is confirmed by increasing nitrogen content. The excess nitrogen can no longer originate from PEI, since the substrate silicon signal is significantly reduced after adsorption. For the CNF films, the amount of nitrogen was clearly increased after adsorption of the block copolymer (from 1.6 (reference) to 5.3 and 8.3% for D_{33}-$EGMA_{137}$ and D_{74}-$EGMA_{17}$, respectively). Moreover, the small standard deviations in the nitrogen concentration further support the assumption of uniform block copolymer adsorption on the cellulosic surfaces. Note the somewhat higher N% value for the D_{74}-$EGMA_{17}$ sample, which contains a large PDMAEMA block.

Compared to the TOCNF reference (0.9%), the amount of nitrogen on the TOCNF films was substantially higher upon adsorption of the block copolymers: 7.2% for D_{33}-$EGMA_{137}$ and 13.1% for D_{74}-$EGMA_{17}$ (see Supporting Information S3 for XPS spectra for TOCNF with adsorbed D_{33}-$EGMA_{137}$ and D_{74}-$EGMA_{17}$ block copolymers). The effect of the larger PDMAEMA segment was again seen as a higher N content for the D_{74}-$EGMA_{17}$ adsorbed on TOCNF as compared to D_{33}-$EGMA_{137}$. The XPS results are in agreement with the QCM-D data, indicating little adsorption of block copolymers on regenerated cellulose, somewhat higher adsorption for CNF films, and a significant adsorption on TOCNF.

Table 3 presents the QCM-D frequency and dissipation changes as well as estimated adsorbed masses by Voigt viscoelastic modeling for the nine PDMAEMA-*b*-POEGMA copolymers adsorbed onto the different cellulose surfaces tested. In most cases, the block copolymer adsorption was almost double on CNF relative to regenerated cellulose films (Table 3). It is also apparent that the adsorbed amounts of block

DOI: 10.1021/acs.jpcb.5b07628
J. Phys. Chem. B 2015, 119, 15275−15286

Table 3. QCM-D Frequency and Dissipation Changes upon Adsorption of PDMAEMA-*b*-POEGMA Copolymers with Differing Block Sizes on Regenerated Cellulose, CNF, and TOCNF Films[a]

block copolymer	surface	ΔF3 (Hz)	ΔD3 (1×10^{-6})	Δm (mg/m^2)
D_{33}-$EGMA_{52}$	reg. cellulose	−8.4	1.2	1.6 ± 1.1
	CNF	−15.0	0.8	2.9 ± 0.4
	TOCNF	86.3	−28.4	N/A
D_{33}-$EGMA_{94}$	reg. cellulose	−5.3	0.8	1.1 ± 0.1
	CNF	−19.3	1.6	3.4 ± 0.2
	TOCNF	−177.5	−46.5	N/A
D_{33}-$EGMA_{137}$	reg. cellulose	−3.3	0.4	0.6 ± 0.2
	CNF	−20.8	1.5	3.6 ± 0.1
	TOCNF	−101.6	−28.1	N/A
D_{58}-$EGMA_{10}$	reg. cellulose	−5.2	0.6	1.0 ± 0.4
	CNF	−8.0	−0.1	1.6 ± 0.4
	TOCNF	−146.2	12.5	N/A
D_{58}-$EGMA_{62}$	reg. cellulose	−4.3	0.7	1.3 ± 0.1
	CNF	−18.2	0.7	3.5 ± 0.3
	TOCNF	77.4	−21.4	N/A
D_{58}-$EGMA_{118}$	reg. cellulose	−4.6	1.0	1.5 ± 0.4
	CNF	−14.8	0.5	2.5 ± 0.9
	TOCNF	−7.2	−9.6	N/A
D_{74}-$EGMA_{17}$	reg. cellulose	−5.5	1.6	1.3 ± 0.3
	CNF	−8.8	0.3	1.6 ± 0.4
	TOCNF	−140.0	7.3	N/A
D_{74}-$EGMA_{54}$	reg. cellulose	−3.6	−3.6	1.3 ± 0.1
	CNF	−12.9	−0.1	2.8 ± 0.2
	TOCNF	92.5	−37.7	N/A
D_{74}-$EGMA_{118}$	reg. cellulose	−6.4	1.0	1.5 ± 0.9
	CNF	−23.7	1.6	3.8 ± 1.5
	TOCNF	−122.3	−7.7	N/A

[a]The adsorbed mass (Δm) was obtained by the Voigt viscoelastic model. The amounts of block copolymer adsorbed on TOCNF are not included due to the effect of water removal, as discussed in the text.

copolymers on regenerated cellulose are approximately the same, ~1 mg/m^2, regardless of the sizes of the PDMAEMA and POEGMA blocks. The adsorption of the block copolymers on CNF films increased with the length of the POEGMA segment. This is explained by the increased POEGMA segment molecular weight, which causes an increase in the amount of bound water, which is detected in QCM-D as a large adsorbed mass. Larsson et al. reported similar results for PDMAEMA−poly(di(ethylene glycol) methyl ether methacrylate) (PDEGMA) block copolymer adsorbed on carboxymethylated CNF.[57]

Expulsion of Coupled Water upon PDMAEMA-*b*-POEGMA Adsorption. The changes in the amount of coupled water upon block copolymer adsorption on TOCNF films were further explored with H_2O/D_2O solvent exchange.[35,38] The QCM-D sensograms corresponding to bare silica crystal and silica crystal carrying spin-coated cellulose nanofibrils are presented in Figure 3. The mass of the fibril layer can be calculated (eq 1) by comparing the fundamental resonance of the silica crystal in air before and after CNF spin-coating. The deposition (spin-coating) of CNF causes a decrease in the fundamental resonance of the crystal, corresponding to a CNF areal mass of 10.2 ± 4.4 mg/m^2. The substantial variation in the calculated mass (standard deviation of ca. 50%) has also been previously observed for similar spin-coated CNF films and can be attributed to the heterogeneity of the CNF suspension.[35]

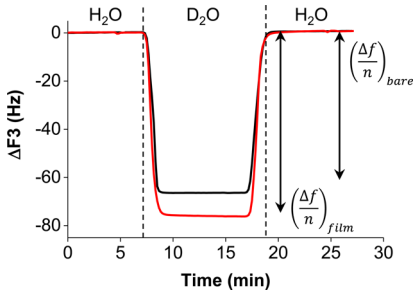

Figure 3. QCM-D third overtone frequency sensogram upon solvent exchange, from H_2O to D_2O and back to H_2O, for bare silica crystal and for a crystal with spin-coated CNF film. Dashed vertical lines indicate the solvent exchange. Double-ended arrows indicate the frequency shifts that were used to calculate the amount of water in the layer by eqs 1 and 2.

H_2O/D_2O solvent exchange experiments were performed for two block copolymers: D_{33}-$EGMA_{137}$ and D_{74}-$EGMA_{54}$ (see Supporting Information S4). These block copolymers were chosen as D_{33}-$EGMA_{137}$ exhibited significant negative changes in the QCM frequency while D_{74}-$EGMA_{54}$ produced substantial positive shifts of QCM frequency. The amount of coupled water in the CNF and TOCNF films was determined to be 60 ± 11 and 63 ± 15%, respectively. Rather surprisingly, TEMPO-oxidation did not significantly increase the amount of water coupling in the cellulose layer, which has been observed when the charge density of CNF is increased with adsorption of carboxymethyl cellulose.[35] The somewhat high variation is caused by the substantial changes in the CNF mass deposited by spin-coating; nevertheless, the results correlate fairly well with previously published data on water content in CNF film.[35] The amount of bound water in the TOCNF layer remained unchanged upon D_{33}-$EGMA_{137}$ adsorption, while in the case of D_{74}-$EGMA_{54}$ a very minor reduction in the amount of coupled water (~4%) was observed. These results can be explained by the decrease in coupled water for block copolymer with the longer cationic segments, thus presenting a higher capacity for charge neutralization. The observed changes are much lower than observed for CNF films and bulk fibers upon cationic polyelectrolyte adsorption (~10−20%);[35,58] water binds extensively to the highly hydrophilic and uncoiled PEG chains of the block copolymers, and they compensate for the water removal caused by charge neutralization by anionic CNF and cationic blocks.

The evidence of interfacial water expulsion upon adsorption of PDMAEMA-*b*-POEGMA on TOCNF was further investigated with SPR. SPR measures the adsorbed layer thickness and mass by determination of the layer refractive index, which is not affected by changes in water coupling. The QCM-D and SPR data upon adsorption on TOCNF of selected PDMAEMA-*b*-POEGMA copolymers is presented in Figure 4.

Depending on the polymer architecture, PDMAEMA−POEGMA block copolymers exhibited either positive or negative shifts in QCM frequency upon adsorption (Figure 4a). Such shifts not only are related to the mass update but are also affected by charge neutralization and water expulsion from the interface (dehydration). In contrast, SPR measurements (Figure 4b) confirmed that all block copolymers in fact adsorbed to a significant extent onto TOCNF. Thus, the adsorption behavior of the block copolymers observed in QCM-D, as anticipated from previous discussions, is indeed a result of water removal

DOI: 10.1021/acs.jpcb.5b07628
J. Phys. Chem. B 2015, 119, 15275−15286

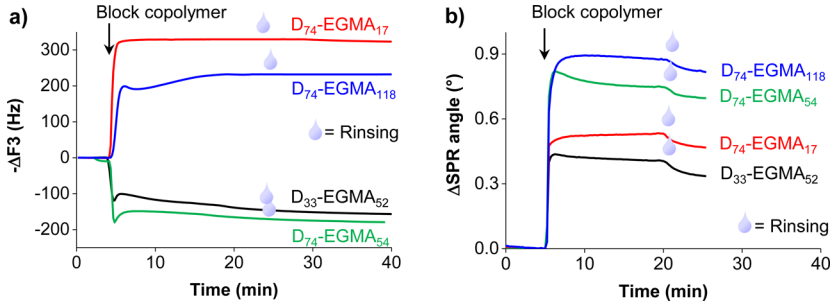

Figure 4. QCM-D (a) and SPR (b) sensograms for adsorption on TOCNF of PDMAEMA-*b*-POEGMA copolymers with varying segment length. The arrows in parts a and b indicate the point when adsorption with respective block copolymer was initiated; droplet symbols indicate rinsing after adsorption plateau with respective buffer solution (pH 6.8).

from the interface, which leads to otherwise unexpected frequency shifts (reduction in frequency).

The adsorption of PDMAEMA-*b*-POEGMA copolymers on TOCNF monitored with SPR (Figure 4b) was very rapid, as the adsorption plateau was reached in a few minutes; rinsing did not remove significant amounts of the copolymers. This is a typical phenomenon for molecules adsorbing by electrostatic interactions.[59] Comparing the adsorption of D_{33}-$EGMA_{52}$ and D_{74}-$EGMA_{54}$, it is evident that adsorption onto TOCNF increases with the size of the PDMAEMA block, likely through more pronounced electrostatic interaction and as a result of the increased entropy as counterions on the surface are displaced by the adsorbing polymer chains. Close comparison of adsorption data for D_{74}-$EGMA_{17}$ and D_{74}-$EGMA_{118}$ reveals an increase with the size of the hydrophilic block. This is similar to the interpretation made from the QCM-D results for block copolymer adsorption on CNF: the adsorbed mass is increased possibly due to the adsorbing PDMAEMA segment, which anchors the rest of the block copolymer with large, dangling POEGMA blocks that bind water extensively.[57] The layer thicknesses calculated from SPR experiments (eq 3) and the adsorbed amount (eq 4) for all nine polymer samples are given in Table 4.

Table 4. Layer Thicknesses and Adsorbed Amounts Calculated from SPR Measurements (eqs 3 and 4) with Standard Deviations for PDMAEMA-*b*-POEGMA Copolymers Adsorbed on TOCNF

block copolymer	d (nm)	Δm (mg/m^2)
D_{33}-$EGMA_{52}$	2.6 ± 0.3	3.0 ± 0.3
D_{33}-$EGMA_{94}$	5.9 ± 0.3	6.8 ± 0.4
D_{33}-$EGMA_{137}$	5.3 ± 0.6	6.1 ± 0.6
D_{58}-$EGMA_{10}$	2.5 ± 0.6	2.9 ± 0.7
D_{58}-$EGMA_{62}$	7.0 ± 0.4	8.1 ± 0.5
D_{58}-$EGMA_{118}$	5.6 ± 1.2	6.4 ± 1.4
D_{74}-$EGMA_{17}$	4.0 ± 0.4	4.6 ± 0.4
D_{74}-$EGMA_{54}$	5.4 ± 0.1	6.2 ± 0.1
D_{74}-$EGMA_{118}$	7.8 ± 0.2	8.9 ± 0.2

The results presented in Table 4 confirm the fact that copolymer adsorption onto TOCNF increases as the size of the PDMAEMA segments increase, due to more prominent electrostatic interactions. The adsorbed amounts of D_{33}-$EGMA_{137}$ and D_{33}-$EGMA_{94}$ were somewhat high compared to the adsorbed amounts of copolymers with 58 or 74 DMAEMA monomers. Since the ionic strength of the phosphate buffer solution (2.5 mM) was relatively low, the electrostatic interactions between the TOCNF surface and PDMAEMA blocks were not screened substantially. The positively charged PDMAEMA blocks adsorbed tightly and in a flat conformation on the anionic surface, while the POEGMA blocks extended to the aqueous medium, as previously observed for poly(L-lysine)–poly(ethylene glycol) graft-copolymers.[60] Therefore, more block copolymers with short PDMAEMA segments fitted the adsorbed layer on the surface compared to block copolymers with longer cationic segments. Also, the large number of POEGMA units in the block copolymer, for a given PDMAEMA block size, were sensed as a large adsorbed mass (Table 4). This is due to the increased mass detected, with highly hydrated polymer chains on the surface of the TOCNF film.[57] It should be noted that, in the case of block copolymers with 33 or 58 DMAEMA monomers, the adsorbed amount first increased with the length of the POEGMA segment (case of D_{33}-$EGMA_{94}$ and D_{58}-$EGMA_{62}$) to then decrease (case D_{33}-$EGMA_{137}$ and D_{58}-$EGMA_{118}$). This is in contrast to the monotonic adsorbed mass increase observed for increased POEGMA segment size for block copolymers carrying 74 DMAEMA monomers. However, the effect highlighted before for block copolymers with 33 or 58 DMAEMA monomers is rather limited and within the reported experimental errors. The heterogeneity of the spin-coated substrate material may be a reason for any unexpected behavior.

Effect of PDMAEMA–POEGMA Copolymer Structure on Adsorption on TEMPO-Oxidized CNF. The SPR sensograms for adsorption on TOCNF of PDMAEMA-*rnd*-POEGMA copolymers with given molecular ratios, D_{46}-$EGMA_{139}$ (10–90 mol %), D_{86}-$EGMA_{67}$ (30–70 mol %), $D_{159}EGMA_{23}$ (70–30 mol %), and $D_{222}EGMA_{7}$ (92–8 mol %) (see Supporting Information S5), both under charged (pH ∼ 6.8) and uncharged (pH 5.5 and pH 9.5) conditions, are presented in Figure 5. From this figure, it is apparent that for all random copolymers adsorption was substantially increased by quaternization. The adsorption isotherms for the charged random copolymers are quite different compared to typical Langmuir adsorption kinetics (Figure 5): after very rapid, initial adsorption, the amount of quaternized polymer levels off with a gradual (but linearly increasing) adsorption rate. It can be assumed that the initial fast adsorption is caused by electrostatic interaction between the quaternized DMAEMA units and the anionic TOCNF. After this, the adsorption rate decreases possibly due to multilayer formation, polymer reconformation on the surface, polymer exchange (between copolymers of different sizes due to their polydispersity), or slow counterion release from the quaternized copolymer layer. In general, adsorption of the charged random copolymers increases when the molecular weight of the polymer and the ratio of OEGMA

DOI: 10.1021/acs.jpcb.5b07628
J. Phys. Chem. B 2015, 119, 15275–15286

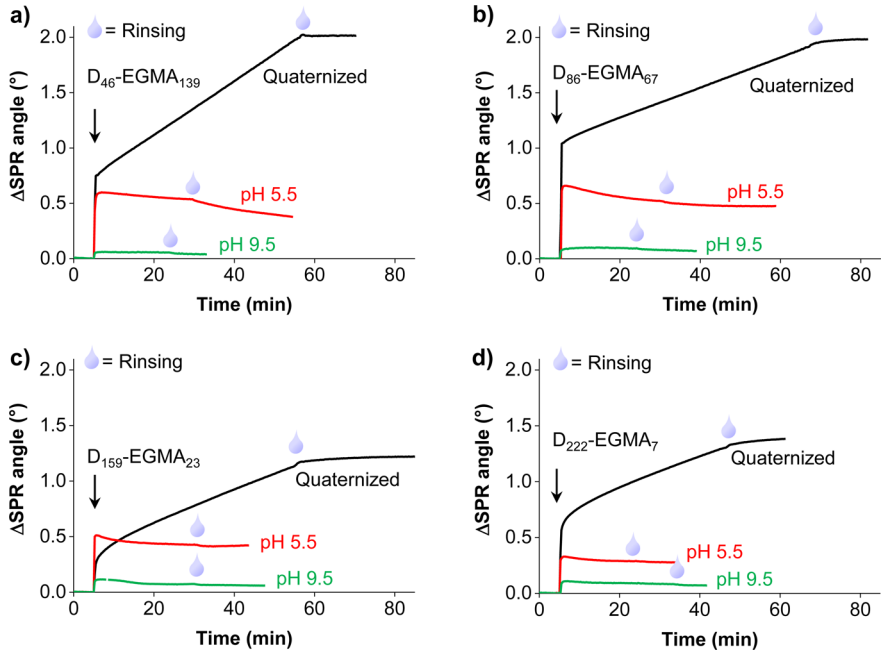

Figure 5. Adsorption on TOCNF of quaternized (pH ~ 6.8) and uncharged (pH 5.5 and 9.5) PDMAEMA-*rnd*-POEGMA copolymers monitored by SPR, as indicated. The arrows symbolize the time when the random copolymer injection was initiated, and the droplet symbols correspond to rinsing with the respective buffer solution.

units is increased: 20.1 ± 1.9 and 12.1 ± 0.9 mg/m^2 for D_{46}-$EGMA_{139}$ (73 kDa, 10−90 mol %) and $D_{159}EGMA_{23}$ (36 kDa, 70−30 mol %), respectively (Supporting Information S6 and S7). This is again due to the higher molecular mass of OEGMA compared to DMAEMA monomer: as the molar mass of the copolymer increases, a higher adsorbed mass is detected.[57]

Interestingly, the adsorption kinetics as well as the adsorbed amount of quaternized PDMAEMA-*rnd*-POEGMA on TOCNF are rather different from that of the respective block copolymers. For all random copolymers after fast initial adsorption, a gradual increasing adsorption is observed (Figure 5), whereas for the block copolymers the adsorption plateau is reached very fast in a few minutes (Figure 4b). As discussed before, the cationic segments of the block copolymers adsorb tightly and flat on the TOCNF surface while the POEGMA chains extend into the solution. However, in the case of the random copolymers, the random DMAEMA segments/monomers on the polymer adsorb on the TOCNF surface while the OEGMA segments extend to the solution, forming loops and tails.

Comparing the adsorbed amounts for random copolymer D_{46}-$EGMA_{139}$ (20.1 ± 1.9 mg/m^2) and block copolymer D_{33}-$EGMA_{137}$ (6.1 ± 0.6 mg/m^2), which have similar molecular ratios and molecular mass (10−90 and 7−93 mol %, and 70 kDa, respectively), it is clear that adsorption on TOCNF is significantly higher for the random copolymer. Overall, the molecular weights of the random copolymers (Supporting Information S5) were somewhat higher than those of the respective block copolymers (Table 1), which can account to some extent for the higher adsorption observed in SPR. However, it is evident that the high adsorption and peculiar adsorption kinetics of the PDMAEMA-*rnd*-POEGMA copolymers on TOCNF still require further investigation.

Nonquaternized copolymers were adsorbed on TOCNF films from acetate (pH 5.5) and carbonate (pH 9.5) buffer solutions (Figure 5), thus allowing us to elucidate the effect of the DMAEMA on adsorption (since it is positively charged when the tertiary amine groups of DMAEMA monomers are protonated in pH 5.5 or deprotonated in pH 9.5 (pK_a 7.4−7.8)).[20] The positive charge of DMAEMA monomers is the main driving force for adsorption on anionic TOCNF, since, as observed, adsorption was significantly higher at pH 5.5. At pH 9.5, adsorption was rather small and of similar magnitude for all random copolymers. The increased amount of OEGMA, as before, is observed to increase adsorption at pH 5.5, similarly as for the charged polymer. If one compares these results for the adsorption of quaternized PDMAEMA−POEGMA and those of random (Figure 5) and block (Figure 4b) polymers, it is evident that quaternization increases adsorption onto TOCNF.

CONCLUSIONS

Quaternized PDMAEMA-*b*-POEGMA copolymer adsorption on regenerated cellulose, CNF, and TOCNF films was studied. By using complementary QCM-D and SPR data, it was determined that block copolymer adsorption on TOCNF and CNF was mainly driven by electrostatic interactions while the increased size of the POEGMA segment had a favorable effect on the sensed adsorbed mass. Very little adsorption occurred on regenerated cellulose films, due to the absence of electrostatic interactions. XPS analysis of the surfaces after block copolymer adsorption further confirms that PDMAEMA-*b*-POEGMA adsorbs to the largest extent on TOCNF and very limited on regenerated cellulose. AFM images revealed that the block copolymers were uniformly attached to the surface, making the fibrillar network features less distinctive.

The block copolymers were found to cause positive and negative QCM-D frequency shifts upon adsorption onto TOCNF, while SPR measurements confirmed a significant adsorption for all block copolymers. Therefore, the removal of interfacial water and their effect upon polymer adsorption is clearly proven. The amount and kinetics of adsorption of similar but random quaternized PDMAEMA−POEGMA copolymers on TOCNF was found to differ substantially from those observed

DOI: 10.1021/acs.jpcb.5b07628
J. Phys. Chem. B 2015, 119, 15275−15286

for respective block copolymers. Compared to quaternized PDMAEMA-*b*-POEGMA, the quaternized, random copolymer samples adsorbed more significantly onto TOCNF.

■ ASSOCIATED CONTENT

Supporting Information

The Supporting Information is available free of charge on the ACS Publications website at DOI: 10.1021/acs.jpcb.5b07628.

In situ TEMPO oxidation of CNF films in QCM-D and SPR, XPS high resolution carbon spectra for regenerated cellulose, CNF, and TOCNF films before and after adsorption of D_{33}-$EGMA_{137}$ and D_{74}-$EGMA_{17}$, H_2O/D_2O solvent exchange QCM-D sensograms for bare silica sensors, cellulose, CNF, and TOCNF films with adsorbed D_{33}-$EGMA_{137}$ or D_{74}-$EGMA_{54}$, characterization information for analyzed PDMAEMA-*rnd*-POEGMA copolymers with given molecular ratios, calculated PDMAEMA-*rnd*-POEGMA copolymer layer thickness, and adsorbed mass on TOCNF (PDF)

■ AUTHOR INFORMATION

Corresponding Author

*Phone: +358 40 3543143. E-mail: hannes.orelma@vtt.fi.

Author Contributions

The manuscript was written through contributions of all authors. All authors have given approval to the final version of the manuscript.

Notes

The authors declare no competing financial interest.

■ ACKNOWLEDGMENTS

The authors are grateful for funding support by the Academy of Finland through its Centres of Excellence Programme (2014−2019), under Project 264677 "Molecular Engineering of Biosynthetic Hybrid Materials Research" (HYBER) and also under the project "Nanocellulose Assemblies for Microsensing and Fluidics" as well as by the WoodWisdom-Net project "Self-Assembled Biomimetic Wood-Based Nanocomposites (Cell-Assembly)". A.W. acknowledges funding from the BMBF in the framework of the Aquamat research group. Prof. Olli Ikkala is acknowledged for valuable comments and Dr. Joseph Campbell for performing XPS measurements. Ritva Kivelä and Anu Anttila are greatly thanked for their technical assistance.

■ REFERENCES

(1) Eichhorn, S.; et al. Review: Current International Research into Cellulose Nanofibres and Nanocomposites. *J. Mater. Sci.* **2010**, *45*, 1−33.

(2) Siqueira, G.; Bras, J.; Dufresne, A. Cellulose Whiskers Versus Microfibrils: Influence of the Nature of the Nanoparticle and its Surface Functionalization on the Thermal and Mechanical Properties of Nanocomposites. *Biomacromolecules* **2009**, *10*, 425−432.

(3) Iwamoto, S.; Isogai, A.; Iwata, T. Structure and Mechanical Properties of Wet-Spun Fibers made from Natural Cellulose Nanofibers. *Biomacromolecules* **2011**, *12*, 831−836.

(4) Turbak, A. F.; Snyder, F. W.; Sandberg, K. R. Microfibrillated Cellulose, a New Cellulose Product: Properties, Uses, and Commercial Potential. *J. Appl. Polym. Sci.: Appl. Polym. Symp.* **1983**, *37*, 815−827.

(5) Jiang, F.; Hsieh, Y. Super Water Absorbing and Shape Memory Nanocellulose Aerogels from TEMPO-Oxidized Cellulose Nanofibrils Via Cyclic Freezing−thawing. *J. Mater. Chem. A* **2014**, *2*, 350−359.

(6) Metreveli, G.; Wågberg, L.; Emmoth, E.; Belák, S.; Strømme, M.; Mihranyan, A. A Size Exclusion Nanocellulose Filter Paper for Virus Removal. *Adv. Healthcare Mater.* **2014**, *3*, 1546−1550.

(7) Arola, S.; Tammelin, T.; Setälä, H.; Tullila, A.; Linder, M. B. Immobilization - Stabilization of Proteins on Nanofibrillated Cellulose Derivatives and their Bioactive Film Formation. *Biomacromolecules* **2012**, *13*, 594−603.

(8) Andresen, M.; Stenstad, P.; Møretrø, T.; Langsrud, S.; Syverud, K.; Johansson, L.; Stenius, P. Nonleaching Antimicrobial Films Prepared from Surface-Modified Microfibrillated Cellulose. *Biomacromolecules* **2007**, *8*, 2149−2155.

(9) Syverud, K.; Stenius, P. Strength and Barrier Properties of MFC Films. *Cellulose* **2009**, *16*, 75−85.

(10) Abe, K.; Iwamoto, S.; Yano, H. Obtaining Cellulose Nanofibers with a Uniform Width of 15 Nm from Wood. *Biomacromolecules* **2007**, *8*, 3276−3278.

(11) Pääkkö, M.; Ankerfors, M.; Kosonen, H.; Nykänen, A.; Ahola, S.; Österberg, M.; Ruokolainen, J.; Laine, J.; Larsson, P. T.; Ikkala, O.; Lindström, T. Enzymatic Hydrolysis Combined with Mechanical Shearing and High-Pressure Homogenization for Nanoscale Cellulose Fibrils and Strong Gels. *Biomacromolecules* **2007**, *8*, 1934−1941.

(12) Saito, T.; Kimura, S.; Nishiyama, Y.; Isogai, A. Cellulose Nanofibers Prepared by TEMPO-Mediated Oxidation of Native Cellulose. *Biomacromolecules* **2007**, *8*, 2485−2491.

(13) Liu, X.; He, F.; Salas, C.; Pasquinelli, M. A.; Genzer, J.; Rojas, O. J. Experimental and Computational Study of the Effect of Alcohols on the Solution and Adsorption Properties of a Nonionic Symmetric Triblock Copolymer. *J. Phys. Chem. B* **2012**, *116*, 1289−1298.

(14) Liu, H.; Li, Y.; Krause, W. E.; Pasquinelli, M. A.; Rojas, O. J. Mesoscopic Simulations of the Phase Behavior of Aqueous EO19PO29EO19 Solutions Confined and Sheared by Hydrophobic and Hydrophilic Surfaces. *ACS Appl. Mater. Interfaces* **2012**, *4*, 87−95.

(15) Li, Y.; Liu, H.; Song, J.; Rojas, O. J.; Hinestroza, J. P. Adsorption and Association of a Symmetric PEO-PPO-PEO Triblock Copolymer on Polypropylene, Polyethylene, and Cellulose Surfaces. *ACS Appl. Mater. Interfaces* **2011**, *3*, 2349−2357.

(16) Liu, X.; Wu, D.; Turgman-Cohen, S.; Genzer, J.; Theyson, T. W.; Rojas, O. J. Adsorption of a Nonionic Symmetric Triblock Copolymer on Surfaces with Different Hydrophobicity. *Langmuir* **2010**, *26*, 9565−9574.

(17) Liu, X.; Vesterinen, A.; Genzer, J.; Seppälä, J. V.; Rojas, O. J. Adsorption of PEO−PPO−PEO Triblock Copolymers with End-Capped Cationic Chains of Poly (2-Dimethylaminoethyl Methacrylate). *Langmuir* **2011**, *27*, 9769−9780.

(18) Nurmi, L.; Kontturi, K.; Houbenov, N.; Laine, J.; Ruokolainen, J.; Seppälä, J. Modification of Surface Wettability through Adsorption of Partly Fluorinated Statistical and Block Polyelectrolytes from Aqueous Medium. *Langmuir* **2010**, *26*, 15325−15332.

(19) Wang, M.; Olszewska, A.; Walther, A.; Malho, J.; Schacher, F. H.; Ruokolainen, J.; Ankerfors, M.; Laine, J.; Berglund, L. A.; Osterberg, M. Colloidal Ionic Assembly between Anionic Native Cellulose Nanofibrils and Cationic Block Copolymer Micelles into Biomimetic Nanocomposites. *Biomacromolecules* **2011**, *12*, 2074−2081.

(20) Van de Wetering, P.; Zuidam, N.; Van Steenbergen, M.; Van der Houwen, O.; Underberg, W.; Hennink, W. A Mechanistic Study of the Hydrolytic Stability of Poly (2-(Dimethylamino) Ethyl Methacrylate). *Macromolecules* **1998**, *31*, 8063−8068.

(21) Filpponen, I.; Kontturi, E.; Nummelin, S.; Rosilo, H.; Kolehmainen, E.; Ikkala, O.; Laine, J. Generic Method for Modular Surface Modification of Cellulosic Materials in Aqueous Medium by Sequential "click" Reaction and Adsorption. *Biomacromolecules* **2012**, *13*, 736−742.

(22) Wang, S.; Guo, X.; Wang, L.; Wang, W.; Yu, Y. Effect of PEG Spacer on Cellulose Adsorbent for the Removal of Low Density Lipoprotein-Cholesterol. *Artif. Cells, Blood Substitutes, Biotechnol.* **2006**, *34*, 101−112.

(23) Olszewska, A.; Junka, K.; Nordgren, N.; Laine, J.; Rutland, M. W.; Österberg, M. Non-Ionic Assembly of Nanofibrillated Cellulose and Polyethylene Glycol Grafted Carboxymethyl Cellulose and the Effect of

DOI: 10.1021/acs.jpcb.5b07628
J. Phys. Chem. B 2015, 119, 15275−15286

Aqueous Lubrication in Nanocomposite Formation. *Soft Matter* **2013**, *9*, 7448−7457.
(24) Braithwaite, G.; Howe, A.; Luckham, P. Interactions between Poly (Ethylene Oxide) Layers Adsorbed to Glass Surfaces Probed by using a Modified Atomic Force Microscope. *Langmuir* **1996**, *12*, 4224−4237.
(25) Maddikeri, R.; Tosatti, S.; Schuler, M.; Chessari, S.; Textor, M.; Richards, R.; Harris, L. Reduced Medical Infection Related Bacterial Strains Adhesion on Bioactive RGD Modified Titanium Surfaces: A First Step Toward Cell Selective Surfaces. *J. Biomed. Mater. Res., Part A* **2008**, *84*, 425−435.
(26) Yan, X.; Perry, S. S.; Spencer, N. D.; Pasche, S.; De Paul, S. M.; Textor, M.; Lim, M. S. Reduction of Friction at Oxide Interfaces upon Polymer Adsorption from Aqueous Solutions. *Langmuir* **2004**, *20*, 423−428.
(27) Drobek, T.; Spencer, N. D. Nanotribology of Surface-Grafted PEG Layers in an Aqueous Environment. *Langmuir* **2008**, *24*, 1484−1488.
(28) Lee, S.; Müller, M.; Heeb, R.; Zürcher, S.; Tosatti, S.; Heinrich, M.; Amstad, F.; Pechmann, S.; Spencer, N. Self-Healing Behavior of a Polyelectrolyte-Based Lubricant Additive for Aqueous Lubrication of Oxide Materials. *Tribol. Lett.* **2006**, *24*, 217−223.
(29) Chawla, K.; Lee, S.; Lee, B. P.; Dalsin, J. L.; Messersmith, P. B.; Spencer, N. D. A Novel Low friction Surface for Biomedical Applications: Modification of Poly (Dimethylsiloxane) (PDMS) with Polyethylene Glycol (PEG)-DOPA-lysine. *J. Biomed. Mater. Res., Part A* **2009**, *90*, 742−749.
(30) VandeVondele, S.; Vörös, J.; Hubbell, J. A. RGD-Grafted Poly-L-Lysine-Graft-(Polyethylene Glycol) Copolymers Block Non-Specific Protein Adsorption while Promoting Cell Adhesion. *Biotechnol. Bioeng.* **2003**, *82*, 784−790.
(31) Isogai, A.; Saito, T.; Fukuzumi, H. TEMPO-Oxidized Cellulose Nanofibers. *Nanoscale* **2011**, *3*, 71−85.
(32) Matthews, J. F.; Skopec, C. E.; Mason, P. E.; Zuccato, P.; Torget, R. W.; Sugiyama, J.; Himmel, M. E.; Brady, J. W. Computer Simulation Studies of Microcrystalline Cellulose Iβ. *Carbohydr. Res.* **2006**, *341*, 138−152.
(33) Driemeier, C.; Bragatto, J. Crystallite Width Determines Monolayer Hydration Across a Wide Spectrum of Celluloses Isolated from Plants. *J. Phys. Chem. B* **2013**, *117*, 415−421.
(34) Mohan, T.; Spirk, S.; Kargl, R.; Doliška, A.; Vesel, A.; Salzmann, I.; Resel, R.; Ribitsch, V.; Stana-Kleinschek, K. Exploring the Rearrangement of Amorphous Cellulose Model Thin Films upon Heat Treatment. *Soft Matter* **2012**, *8*, 9807−9815.
(35) Kontturi, K. S.; Kontturi, E.; Laine, J. Specific Water Uptake of Thin Films from Nanofibrillar Cellulose. *J. Mater. Chem. A* **2013**, *1*, 13655−13663.
(36) Wågberg, L.; Decher, G.; Norgren, M.; Lindström, T.; Ankerfors, M.; Axnäs, K. The Build-Up of Polyelectrolyte Multilayers of Microfibrillated Cellulose and Cationic Polyelectrolytes. *Langmuir* **2008**, *24*, 784−795.
(37) Craig, V. S.; Plunkett, M. Determination of Coupled Solvent Mass in Quartz Crystal Microbalance Measurements using Deuterated Solvents. *J. Colloid Interface Sci.* **2003**, *262*, 126−129.
(38) Kittle, J. D.; Du, X.; Jiang, F.; Qian, C.; Heinze, T.; Roman, M.; Esker, A. R. Equilibrium Water Contents of Cellulose Films Determined Via Solvent Exchange and Quartz Crystal Microbalance with Dissipation Monitoring. *Biomacromolecules* **2011**, *12*, 2881−2887.
(39) Rodahl, M.; Kasemo, B. A Simple Setup to Simultaneously Measure the Resonant Frequency and the Absolute Dissipation Factor of a Quartz Crystal Microbalance. *Rev. Sci. Instrum.* **1996**, *67*, 3238−3241.
(40) Schasfoort, R. B. M., Tudos, A. J., Eds. *Handbook of surface plasmon resonance*; Royal Society of Chemistry: Cambridge, U.K., 2008.
(41) Cooper, G. K.; Sandberg, K. R.; Hinck, J. F. Trimethylsilyl Cellulose as Precursor to Regenerated Cellulose Fiber. *J. Appl. Polym. Sci.* **1981**, *26*, 3827−3836.
(42) Kontturi, E.; Thüne, P. C.; Niemantsverdriet, J. W. Cellulose Model Surfaces - Simplified Preparation by Spin Coating and Characterization by X-Ray Photoelectron Spectroscopy, Infrared Spectroscopy, and Atomic Force Microscopy. *Langmuir* **2003**, *19*, 5735−5741.
(43) Ahola, S.; Salmi, J.; Johansson, L.; Laine, J.; Österberg, M. Model Films from Native Cellulose Nanofibrils. Preparation, Swelling, and Surface Interactions. *Biomacromolecules* **2008**, *9*, 1273−1282.
(44) Rodahl, M.; Hook, F.; Krozer, A.; Brzezinski, P.; Kasemo, B. Quartz Crystal Microbalance Setup for Frequency and Q-Factor Measurements in Gaseous and Liquid Environments. *Rev. Sci. Instrum.* **1995**, *66*, 3924−3930.
(45) Sauerbrey, G. The use of Quartz Oscillators for Weighing Thin Layers and for Microweighing. *Eur. Phys. J. A* **1959**, *155*, 206−222.
(46) Rodahl, M.; Kasemo, B. On the Measurement of Thin Liquid Overlayers with the Quartz-Crystal Microbalance. *Sens. Actuators, A* **1996**, *54*, 448−456.
(47) Voinova, M. V.; Rodahl, M.; Jonson, M.; Kasemo, B. Viscoelastic Acoustic Response of Layered Polymer Films at Fluid-Solid Interfaces: Continuum Mechanics Approach. *Phys. Scr.* **1999**, *59*, 391.
(48) Kittle, J. D.; Wondraczek, H.; Wang, C.; Jiang, F.; Roman, M.; Heinze, T.; Esker, A. R. Enhanced Dewatering of Polyelectrolyte Nanocomposites by Hydrophobic Polyelectrolytes. *Langmuir* **2012**, *28*, 11086−11094.
(49) Zwolinski, B. J.; Eicher, L. D. High-Precision Viscosity of Supercooled Water and Analysis of the Extended Range Temperature Coefficient. *J. Phys. Chem.* **1971**, *75*, 2016−2024.
(50) Lide, D. R., Ed. *Handbook of Chemistry and Physics*; CRC Press: Boca Raton, FL, 1992; p 1.
(51) Jung, L. S.; Campbell, C. T.; Chinowsky, T. M.; Mar, M. N.; Yee, S. S. Quantitative Interpretation of the Response of Surface Plasmon Resonance Sensors to Adsorbed Films. *Langmuir* **1998**, *14*, 5636−5648.
(52) Campbell, C. T.; Kim, G. SPR Microscopy and its Applications to High-Throughput Analyses of Biomolecular Binding Events and their Kinetics. *Biomaterials* **2007**, *28*, 2380−2392.
(53) Lee, B. S.; Chi, Y. S.; Lee, K.; Kim, Y.; Choi, I. S. Functionalization of Poly(Oligo(Ethylene Glycol) Methacrylate) Films on Gold and Si/SiO2 for Immobilization of Proteins and Cells: SPR and QCM Studies. *Biomacromolecules* **2007**, *8*, 3922−3929.
(54) Feng, W.; Zhu, S.; Ishihara, K.; Brash, J. Protein Resistant Surfaces: Comparison of Acrylate Graft Polymers Bearing Oligo-Ethylene Oxide and Phosphorylcholine Side Chains. *Biointerphases* **2006**, *1*, 50−60.
(55) Johansson, L.; Campbell, J. Reproducible XPS on Biopolymers: Cellulose Studies. *Surf. Interface Anal.* **2004**, *36*, 1018−1022.
(56) Sjöström, E. The Origin of Charge on Cellulosic Fibers. *Nord. Pulp Pap. Res. J.* **1989**, *4*, 90−93.
(57) Larsson, E.; Sanchez, C. C.; Porsch, C.; Karabulut, E.; Wågberg, L.; Carlmark, A. Thermo-Responsive Nanofibrillated Cellulose by Polyelectrolyte Adsorption. *Eur. Polym. J.* **2013**, *49*, 2689−2696.
(58) Swerin, A.; Ödberg, L.; Lindström, T. Deswelling of Hardwood Kraft Pulp Fibres by Cationic Polymers. the Effect on Wet Pressing and Sheet Properties. *Nord. Pulp Pap. Res. J.* **1990**, *5*, 188−196.
(59) Hoogeveen, N. G.; Stuart, M. A. C.; Fleer, G. J. Polyelectrolyte Adsorption on Oxides: II. Reversibility and Exchange. *J. Colloid Interface Sci.* **1996**, *182*, 146−157.
(60) Kenausis, G. L.; Vörös, J.; Elbert, D. L.; Huang, N.; Hofer, R.; Ruiz-Taylor, L.; Textor, M.; Hubbell, J. A.; Spencer, N. D. Poly (L-Lysine)-G-Poly (Ethylene Glycol) Layers on Metal Oxide Surfaces: Attachment Mechanism and Effects of Polymer Architecture on Resistance to Protein Adsorption. *J. Phys. Chem. B* **2000**, *104*, 3298−3309.

DOI: 10.1021/acs.jpcb.5b07628
J. Phys. Chem. B 2015, 119, 15275−15286